A Journal of the Gesellschaft Deutscher Chemiker

Angewandte International Edition GDCh Chemie

www.angewandte.org

Accepted Article

Title: Rhodium-Catalyzed Enantioselective Formal [4+1] Cyclization of Benzyl Alcohols and Benzaldimines: Facile Access to Silicon-Stereogenic Heterocycles

Authors: Bingxue Shen, Deng Pan, Wanying Xie, Xiao-Xi Li, Songjie Yu, Genping Huang, and Xingwei Li

To be cited as: *Angew. Chem. Int. Ed.* **2023**, e202315230

Link to VoR: https://doi.org/10.1002/anie.202315230

WILEY VCH

10.1002/anie.202315230

RESEARCH ARTICLE

WILEY VCH

Rhodium-Catalyzed Enantioselective Formal [4+1] Cyclization of Benzyl Alcohols and Benzaldimines: Facile Access to Silicon-Stereogenic Heterocycles

Bingxue Shen,[a] Deng Pan,[b] Wanying Xie,[a] Xiao-Xi Li,[a] Songjie Yu,[a]* Genping Huang,[b]* Xingwei Li[a,c]*

Dedication ((optional))

[a] B. Shen, W. Xie, Dr. X.-X. Li, Prof. Dr. S. Yu. Prof. Dr. X. Li
Institute of Molecular Sciences and Engineering, Institute of Frontier and Interdisciplinary Science
Shandong University, Qingdao 266237, China
E-mail: yusongjie08@mails.ucas.ac.cn; lixw@snnu.edu.cn

[b] D. Pan, Prof. Dr. G. Huang
Department of Chemistry, School of Science and Tianjin Key Laboratory of Molecular Optoelectronic Sciences
Tianjin University, Tianjin 300072, China
Email: gphuang@tju.edu.cn

[c] Prof. Dr. X. Li
School of Chemistry and Chemical Engineering
Shaanxi Normal University, Xi'an 710062, China

Supporting information for this article is given via a link at the end of the document.

Abstract: The carbon-to-silicon switch in formation of bioactive sila-heterocycles with a silicon-stereogenic center has garnered significant interest in drug discovery. However, metal-catalyzed synthesis of such scaffolds is still in its infancy. Herein, a rhodium-catalyzed enantioselective formal [4+1] cyclization of benzyl alcohols and benzaldimines has been realized by enantioselective difunctionalization of a secondary silane reagent, affording chiral-at-silicon cyclic silyl ethers and sila-isoindolines, respectively. Mechanistic studies reveal a dual role of the rhodium-hydride catalyst. The coupling system proceeds via rhodium-catalyzed enantio-determining dehydrogenative OH silylation of the benzyl alcohol or hydrosilylation of the imine to give an enantioenriched silyl ether or silazane intermediate, respectively. The same rhodium catalyst also enables subsequent intramolecular cyclative C−H silylation directed by the pendent Si−H group. Experimental and DFT studies have been conducted to explore the mechanism of the OH bond silylation of benzyl alcohol, where the Si-O reductive elimination from a Rh(III) hydride intermediate has been established as an enantiodetermining step.

Introduction

The silicon element has found ever-increasing applications in medicinal chemistry.[1] The strategic incorporation of a silicon bioisostere into biologically active scaffolds delivers enhanced pharmacokinetic properties such as better cell penetration, bioactivity, and lower toxicity due to its larger covalent radius and lower electronegativity in comparison to the carbon atom.[2] Given these advantages, the carbon−silicon switching constitutes an emerging strategy for the construction of new pharmaceutical candidates (Figure 1).[3] On the other hand, enantioenriched heterocycles are widely present in a large number of drug molecules.[4] However, embedding a enantioenriched silicon bioisostere into such heterocyclic skeletons to ameliorate their pharmacokinetic profiles represents a long-standing challenge, which is ascribed to the extra 3d orbital of silicon center that can interact with heteroatom or metal center to form five- or six-coordinated silicon intermediate, leading to decomposition of silacycles.[5] Therefore, the development of novel strategies to assemble reactive stereogenic silacycles has recently aroused increasing attention.

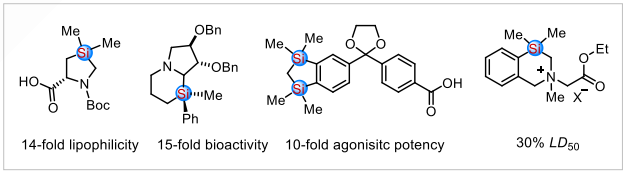

Figure 1. Intrinsic activity and efficacy comparison of the representative silacycles and their all-carbon analogues.

Among the established approaches, metal-catalyzed enantioselective C−H silylation[6] has offered advantageous avenues to access enantioenriched silacycles. In 2013, Takai and Kuninobu *et al.* reported the first enantioselective silylation of sp^2 C−H bonds through a rhodium-catalyzed dehydrogenation, affording enantioenriched spirosilabifluorenes.[7] In 2015, Shibata,[8] He,[9] and Takai[10] groups independently developed rhodium-catalyzed enantioselective silylations of sp^2 C−H bonds to generate planarly chiral ferrocenes. Inspired by these seminal studies, rhodium-, and iridium-catalyzed C−H silylations to forge a diverse range of silacycles containing *C*- and/or *Si*-centered chirality has been increasingly explored (Scheme 1 a).[11] Despite the progress on intramolecular C−H silylations, access to such enantioenriched skeletons is hampered by the tedious pre-installation of silicon groups into functionalized starting materials. Moreover, the ring elements in current enantioenriched silacyclic scaffolds are mostly limited to carbon and silicon. Construction

of chiral sila-*O*-heterocycles and sila-*N*-heterocycles is currently underdeveloped. Hence, it is desirable to develop synthetically useful approaches to forge chiral silacyclic scaffolds with heteroatoms such as oxygen or nitrogen via enantioselective transformations of readily available reagents, which serves to expand the applications of silicon chemistry. In this context, in 2015, Hartwig group disclosed the synthesis of enantioenriched sila-*O*-heterocycles via a bimetallic relay catalysis,[12] where an iridium-catalyzed hydrosilylation of readily available benzophenones occurred first, followed by a rhodium-catalyzed enantioselective silylation of sp^2 C−H bonds directed by the resulting silyl ether (Scheme 1b, left). In 2018, Zhao *et al.* developed an iridium-catalyzed OH silylation of 2-ferrocenyl-substituted phenol and subsequent rhodium-catalyzed

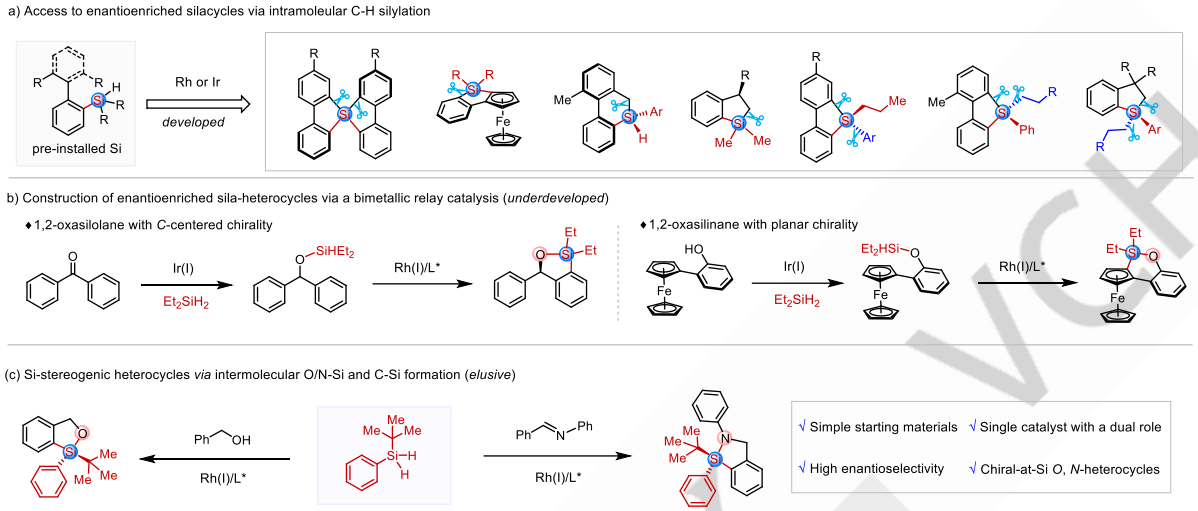

Scheme 1. Catalytic construction of enantioenriched silacycles.

asymmetric dehydrogenative C−H silylation of the resultant silyl ether, forming enantioenriched planarly chiral ferrocenes fused to a six-membered silacycles (Scheme 1b, right).[13] However, all these intermolecular enantioselective C-H silylation systems have been catalyzed by well-tailored sequential bimetallic catalysis, affording only carbon-based central or planar chirality. To date, the synthesis of sila-*O*- and sila-*N*-heterocycles with silicon-stereogenic centers remains elusive. With the goal of potential adoption of silicon-stereogenic *N*- or *O*-heterocyclic molecules, we set out to develop expedient routes from readily available substrates such as benzyl alcohols and benzaldimines. Ideally, the two-step coupling sequence is streamlined by a single catalyst. Inspired by the precedents of metal-catalyzed dehydrogenative alkoxylation of sterically bulky silanes[14] and dehydrogenative Si−C couplings,[15] our conceptual design boils down to developing a compatible transition metal catalyst with a dual role that can both induce Si-chirality in silicon-heteroatom (O and N) coupling and render the subsequent intramolecular dehydrogenative C−Si coupling (Scheme 1c). This is challenging due to the over-alkoxylation of secondary silane, unfavorable intramolecular cyclization of the bulky silicon center as well as the decomposition of aza-silacycle caused by hydrolysis. We now report a novel rhodium-catalyzed highly chemo- and enantioselective synthesis of Si-chiral heterocycles via annulative coupling of benzyl alcohols and benzaldimines with dihydrosilanes.

Results and Discussion

Table 1. Optimization studies.[a]

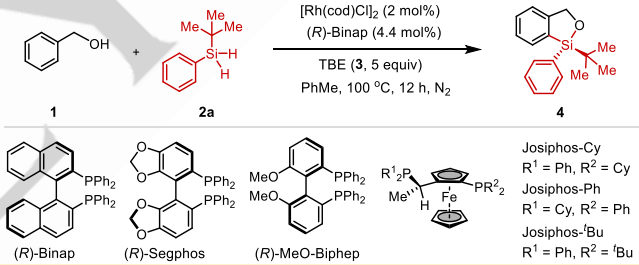

Entry	Variations from standard conditions	Yield/%[b]	e.r./%[c]
1	none	67	23:77
2	(*R*)-Segphos	58	21:79
3	(*R*)-OMe-Biphep	62	21:79
4	Josiphos-Cy	72	88:12
5	Josiphos-Ph	35	53:47
6	Josiphos-^{t}Bu	45	65:35
7	Josiphos-Cy, *m*-xylene	53	90:10
8	Josiphos-Cy, CyH	85	94:6
9	Josiphos-Cy, *n*-hexane	79	95:5
10	$[Rh(coe)_2Cl]_2$, Josiphos-Cy, *n*-hexane	81	97:3
11	$[Rh(C_2H_4)_2Cl]_2$, Josiphos-Cy, *n*-hexane	83	96:4
12	Josiphos-Cy, *n*-hexane, no TBE	< 5	-

[a] benzyl alcohol (0.1 mmol), silane (0.12 mmol), TBE (0.5 mmol), Rh catalyst (2 mol%), chiral ligand (4.4 mol%), solvent (1 mL), nitrogen atmosphere, and 100 °C for 24 h. [b] Isolated yield. [c] e.r. determined by HPLC on a chiral stationary phase.

We initiated our studies by developing the reaction conditions of asymmetric OH silylation-cyclization of benzyl alcohol **1** with *tert*-butyl(phenyl)silane **2a** in the presence of a Rh(I) catalyst (Table 1). We reasoned that an electron-rich

diphosphine ligand with a high *trans* effect would favor Si−H oxidative addition and extrusion of dihydrogen. Several chiral diphosphine ligands were then tested in toluene at 100 °C (entries 1−6) with *tert*-butylethylene (TBE, **3**) as a hydrogen acceptor. The employment of $[Rh(cod)Cl]_2$ (2 mol%) as a catalyst and Josiphos-Cy (4.4 mol%) as a chiral ligand successfully afforded the desired Si-stereogenic cyclic silyl ether **4** in 72% yield with promising enantiocontrol (88:12 e.r., entry 4). Investigation of other common solvents in the presence of Josiphos-Cy ligand revealed that hydrocarbon solvents such as CyH and *n*-hexane gave good yields and superior enantioselectivities (entries 8 and 9). Other Rh(I) olefin catalysts including $[Rh(C_2H_4)_2Cl]_2$ and $[Rh(coe)_2Cl]_2$ delivered the desired product with a slight improvement of enantioselectivities (entries 10 and 11). Specifically, the reaction failed to deliver the cyclic silyl ether product when the TBE was omitted (entry 12). Thus, the reaction conditions outlined in entry 10 (condition A) were retained for further studies.

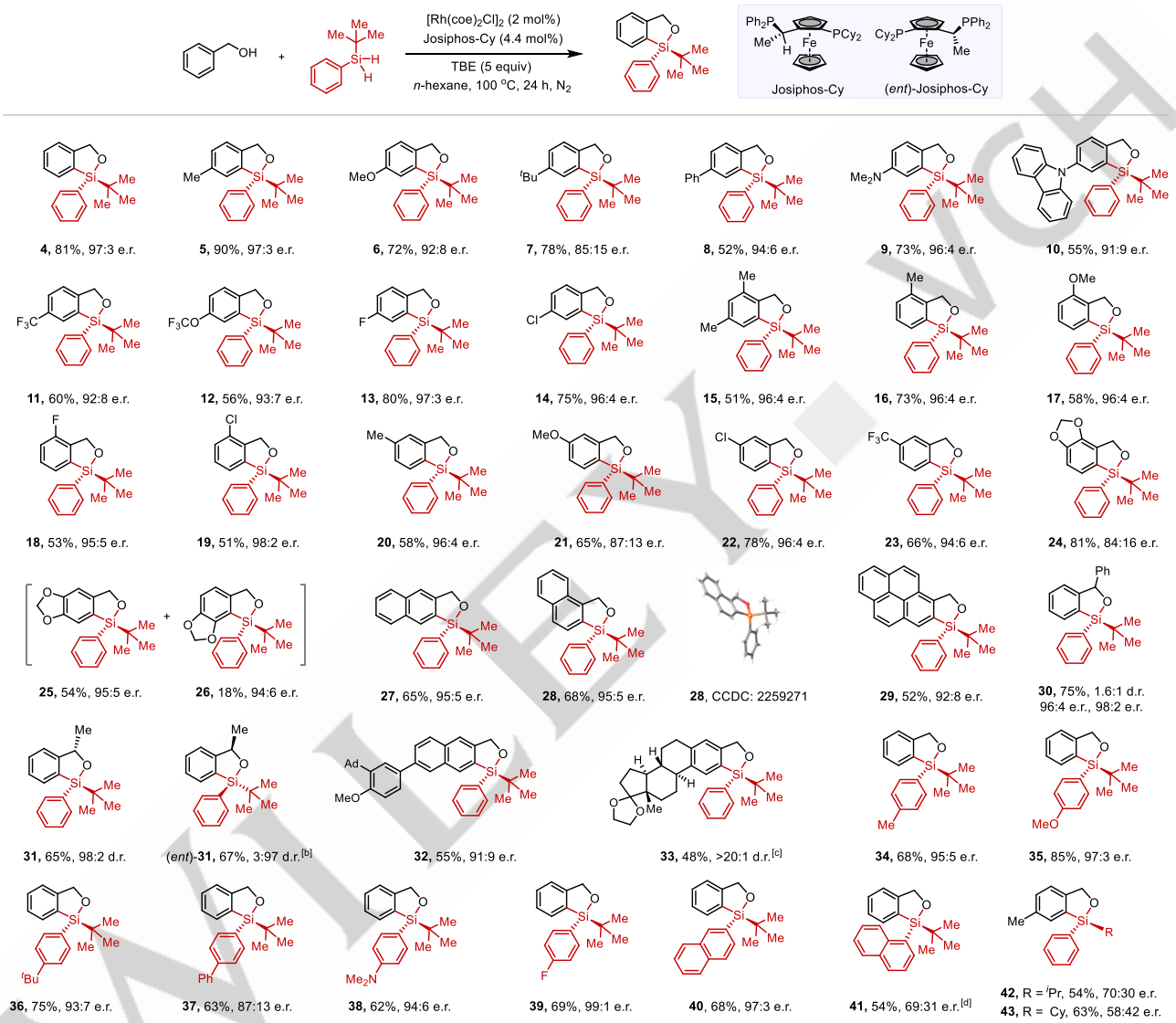

Scheme 2. Scope of benzyl alcohols. [a] benzyl alcohol (0.1 mmol), dihydrosilane (0.12 mmol), TBE (0.5 mmol), $[Rh(coe)_2Cl]_2$ (2 mol%), Josiphos-Cy (4.4 mol%), *n*-hexane (1 mL), nitrogen atmosphere, and 100 °C for 24 h. Isolated yield. [b] (*ent*)-Josiphos-Cy ligand. [c] The d.r. was determined by ^{1}H NMR analysis. [d] 110 °C.

With the optimized reaction conditions in hand, we next examined the scope and generality of this intermolecular [4+1] cyclization system (Scheme 2). A broad scope of benzyl alcohols bearing various electron-donating (Me, OMe, ^{t}Bu, NMe_2, and carbazole), electron-withdrawing (Ph, CF_3 and OCF_3), and halogen (F and Cl) substituents underwent the smooth couplings with *tert*-butyl(phenyl)-silane in generally good to excellent yields (**4**−**14**, 52−90%) with generally high enantioselectivities (85:15−97:3 e.r.). Benzyl alcohols bearing *ortho*-Me, -OMe, -F, and -Cl substituents were also compatible (**15**−**19**), indicating tolerance of steric hindrance. In the case of *meta*-substituted (Me, OMe, Cl, and CF_3) benzyl alcohols, the less hindered C−H site was functionalized (**20**−**24**). When 3,4-(methylenedioxy)benzyl alcohol was used, the reaction gave a mixed product in a 3:1 regioisomeric ratio (**25** and **26**). Aside from the C−H silylation of benzene rings, naphthalene and pyrene rings were also viable (**27**−**29**). The absolute configuration of product **28** was determined by X-ray crystallography (CCDC 2259271),[16] and the rest products were assigned by analogy. Monoaryl and alkyl substituents at the α-

position of the benzyl alcohols were also tolerated. For example, diphenylmethanol reacted to afford the cyclic silyl ether **30** in a good yield with excellent silicon-chirality (96:4 e.r. and 98:2 e.r.), albeit with a low d.r. (1.6:1). The employment of optically pure (*S*)-1-phenylethanol afforded the product **31** with an excellent diastereoselectivity (98:2 d.r.) under the standard reaction conditions, while only a moderate diastereoselectivity (20:80 d.r.) was obtained when using the mirror image ligand (*ent*)-Josiphos-Cy. Accordingly, the (*R*)-1-phenylethanol was better matched with the (*ent*)-Josiphos-Cy ligand, giving (*ent*)-**31** with a 3:97 d.r. ratio. Complex substrates derived from adapalene (**32**) and estrone (**33**) also reacted to give the corresponding products in 55% yield with 91:9 e.r. and 48% yield with an excellent diastereoselectivity, respectively. Furthermore, secondary silanes bearing different functional groups in the benzene ring, including electron-donating (Me, OMe, and ^{t}Bu, **34**−**36**), phenyl (**37**), amino group (**38**), halogen (**39**), and naphthyl groups (**40**), all reacted smoothly with benzyl alcohol in moderate to high yields (62−85%) with good to excellent enantioselectivities (87:13−99:1 e.r.). It should be noted that *tert*-butyl(naphthalen-1-yl)silane only coupled to give the uncyclized silyl ether at 100 °C. While increasing the reaction temperature to 110 °C did improve the cyclization reactivity, the enantioselectivity was low (**41**, 68:32 e.r.). Switching the ^{t}Bu group to less bulky groups including ^{i}Pr and Cy on the dihydrosilane afforded the corresponding products in good yields (54% and 63%), but dramatically reduced enantioselectivities were obtained (**42** and **43**).

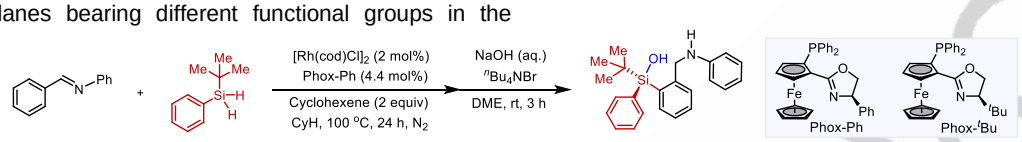

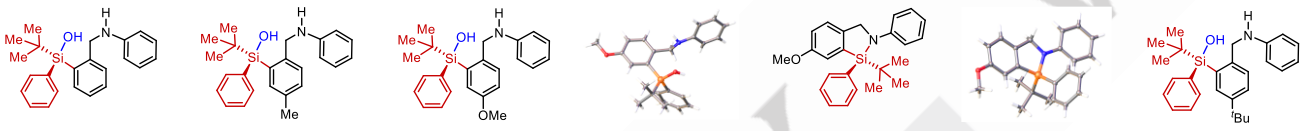
44, 73%, 97:3 e.r.

45, 62%, 97:3 e.r.

46, 65%, 94:6 e.r.

46, CCDC: 2259269

47, 48%, 93:7 e.r.

47, CCDC: 2259272

48, 65%, 96:4 e.r.

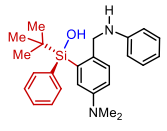
49, 66%, 94:6 e.r.

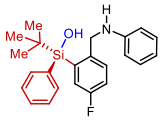
50, 57%, 97:3 e.r.

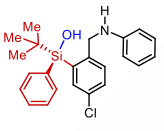
51, 63%, 94:6 e.r.[b]

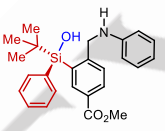
52, 62% yield, 95:5 e.r.[b]

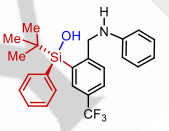
53, 55%, 94:6 e.r.[b]

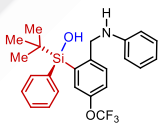
54, 61%, 96:4 e.r.[b]

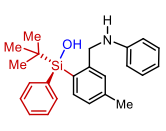
55, 52%, 90:10 e.r.

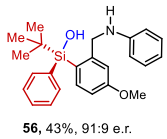
56, 43%, 91:9 e.r.

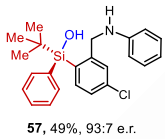
57, 49%, 93:7 e.r.

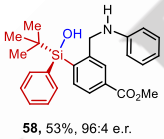
58, 53%, 96:4 e.r.

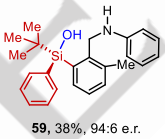
59, 38%, 94:6 e.r.

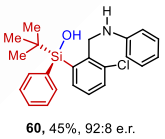
60, 45%, 92:8 e.r.

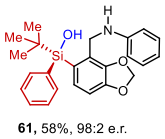
61, 58%, 98:2 e.r.

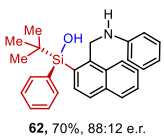
62, 70%, 88:12 e.r.

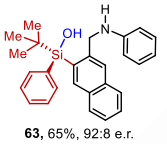
63, 65%, 92:8 e.r.

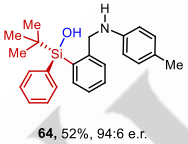
64, 52%, 94:6 e.r.

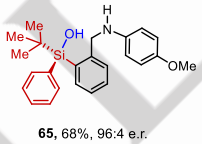
65, 68%, 96:4 e.r.

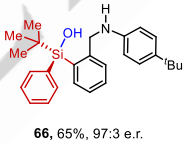
66, 65%, 97:3 e.r.

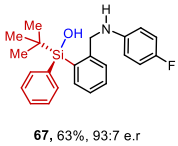
67, 63%, 93:7 e.r

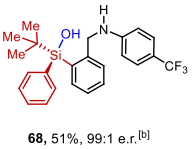
68, 51%, 99:1 e.r.[b]

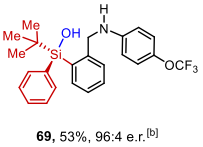
69, 53%, 96:4 e.r.[b]

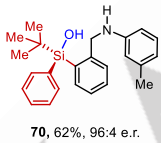
70, 62%, 96:4 e.r.

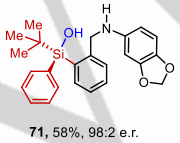
71, 58%, 98:2 e.r.

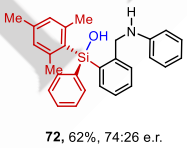
72, 62%, 74:26 e.r.

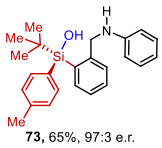
73, 65%, 97:3 e.r.

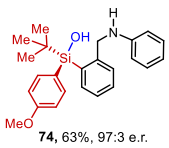
74, 63%, 97:3 e.r.

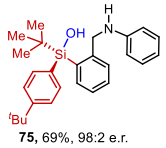
75, 69%, 98:2 e.r.

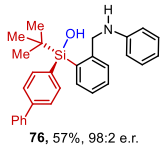
76, 57%, 98:2 e.r.

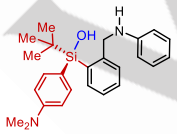
77, 54%, 97:3 e.r.

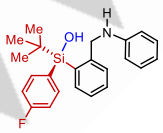
78, 63%, 96:4 e.r.

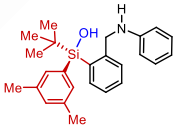
79, 52%, 99:1 e.r.

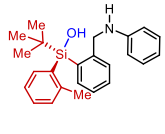
80, 44%, 91:9 e.r.

81, 35%, 98:2 e.r.

82, 49%, 97:3 e.r.

83, 58%, 88:12 e.r.

84, 45%, 94:6 e.r.

85, 34%, 61:39 e.r.

86, 43%, 58:42 e.r.

87, 64%, 73:27 e.r.

Scheme 3. Scope of the dehydrogenative C−H silylation-hydrolysis of benzaldimines. [a] benzaldimine (0.1 mmol), silane (0.12 mmol), cyclohexene (0.2 mmol), $[Rh(cod)Cl]_2$ (2 mol%), Phox-Ph (4.4 mol%), CyH (1 mL), nitrogen atmosphere, and 100 °C for 24 h, followed by treatment with NaOH (aq.)/TBAB in DME. Isolated yield over two steps. [b] Phox-^{t}Bu as a chiral ligand.

To broaden the application of this novel catalytic strategy, diverse *N*-substituted benzyl amines have been extensively attempted under various reaction conditions, but all failed to give any desired coupling product, possibly due to the challenges in the formation of an unstable Si−N bond.[17] Fortunately, switching to *N*-phenyl benzaldimine as a substrate afforded the [4+1] annulative product. Screening of a large set of chiral ligands revealed the superiority of Phox ligand. 59% Yield of desired product **44** with 97:3 e.r. and 59% yield of desired product **44** with 96:4 e.r. were realized respectively when Phox-Ph or Phox-^{t}Bu ligand was used in the presence of cyclohexene as a hydrogen acceptor in cyclohexane (condition B, details in the Supporting Information). Of note, the [4+1] annulated product was prone to hydrolysis, and was silica gel-unstable. Consequently, it was converted to the silanol upon treatment with NaOH/TBAB or TBAOH,[18] where complete inversion of stereochemistry was observed (Scheme 3). We next explored the substrate scope of the coupling of *N*-aryl benzaldimines (Scheme 3). Benzaldimines bearing diverse substituents in the arene rings, such as electron-donating (Me, OMe, ^{t}Bu, and NMe_2), -withdrawing (ester, CF_3, and OCF_3), and halogen (F and Cl) groups, were all viable, affording the corresponding products in moderate to good yields with excellent enantioselectivities (**45**−**61,** 93:7−97:3 e.r.). Besides, naphthylimines were also applicable, albeit with attenuated enantioselectivities (**62,** 88:12 e.r. and **63,** 92:8 e.r.). The absolute configuration of sila-isoindoline intermediate **47** (CCDC 2259272) and the ring-opened silanol product **46** (CCDC 2259269) were both confirmed by X-ray crystallographic analysis, which demonstrated the inversion of stereochemistry. Besides, diverse substituents in the *N*-arene rings were also well tolerated (**64**−**71**, 94:6−99:1 e.r.). The silane substrates were then examined. While mesityl(phenyl)silane only gave a moderate enantioselectivity (**72**, 74:26 e.r.) due to the less pronounced steric bias, other dihydrosilanes bearing different functional groups, including electron-donating groups (Me, OMe, and ^{t}Bu) (**73**−**75**), phenyl (**76**), amino group (**77**), halogen (**78**), or a relatively bulky aryl groups (**79**−**84**), all reacted smoothly with *N*-phenyl-benzaldimine to afford the silanol products in moderate to good two-step yields (35−69%) with high enantioselectivies (88:12−99:1 e.r.). In line with the steric effect in the coupling of dihydrosilanes and benzyl alcohols, the employment of less bulky groups including ^{i}Pr and Cy in the dihydrosilane only afforded the desired products in moderate yields and low enantioselectivies (**85** and **86**). To our surprise, *N*-phenyl-benzaldimine bearing an *ortho*-OMe group underwent silylation at the methyl position rather than the *ortho* position (**87**, 73:27 e.r.).[19]

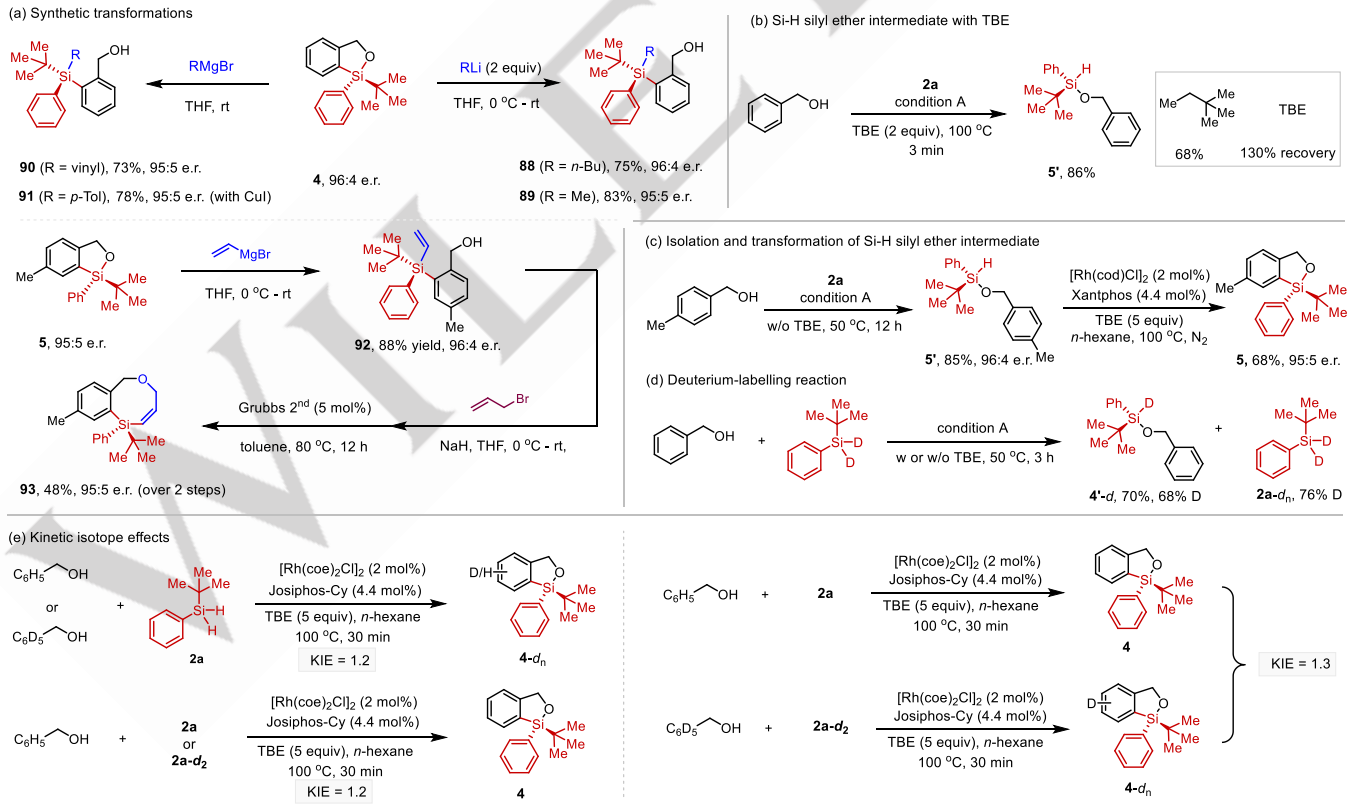

Scheme 4. Synthetic transformations and mechanistic studies.

The synthetic transformations of a chiral silyl ether (*R*)-**4** have been demonstrated in C−C coupling with a series of organometallic reagents (Scheme 4a). The employment of different organolithium reagents afforded the corresponding tetrasubstituted silanes bearing a pendent benzyl alcohol moiety in high yields (**88** and **89**, Scheme 4a). A vinyl Grignard reagent was also compatible (**90**). In all these cases, essentially no erosion of the enantiopurity was detected. In contrast, an aryl

Grignard reagent only reacted with poor efficiency. Fortunately, introduction of CuI additive improved the reactivity (**91**). Analyses of the absolute configuration of the vinyl silane product (**90**) confirmed retention of the silicon chirality. In stark contrast, treatment of the aza-silacycle with NaOH/TBAB results in full inversion of the stereochemistry (Schemes 3 and 4). This discrepancy is rationalized by different mechanisms during the formation of a five-coordinated Si-intermediate. In the case of Me−Li addition, chelation effect of the ethereal oxygen directs the attack of the lithium reagent from the same side, which eventually leads to retention of the stereocenter. In contrast, the low Lewis acidity of the cation in NaOH/TBAB results in backside addition of the hydroxide, leading to eventual inversion of the Si configuration (see the Supporting Information). By taking advantage of the substitution by a Grignard reagent, a further transformation of compound **92** *via* sequential allylation and ring-closure metathesis gave an interesting 8-membered silacycle **93** in high enantioselectivity.

A series of experimental studies have been conducted to gain insight into the mechanism of the coupling of benzylic alcohol (Scheme 4). Performing the reaction in the presence of TBE (2 equiv) for 3 min resulted in the formation of silyl ether intermediate **5'** in 86% yield as well as 2,2-dimethylbutane in 68% yield (Scheme 4b),[20] which demonstrates both the hydrogen acceptance by TBE and extrusion of dihydrogen are competitive pathways in the uncyclized silyl ether formation stage. Indeed, the coupling of *p*-tolylmethanol and silane **2a** occurred in a high yield under mild conditions[21] even in the absence of the hydrogen acceptor to afford an *O*-silylated compound **5'** in a good yield with an excellent enantioselectivity (Scheme 4c, 96:4 e.r.), where essentially the same yield and enantioselectivity were observed whether the hydrogen acceptor was used or not. The absolute configuration of compound **5'** has been determined on the basis of He's report.[14] Subjection of **5'** to the standard conditions or even to catalytic conditions using an achiral Xantphos ligand all afforded the cyclized product **5** in good yields with only slight erosion of enantiopurity (Scheme 4c), where the TBE proved necessary to ensure reactivity. These observations suggest the intermediacy of the silyl ether **5'**, and such an OH silylation event is enantio-determining. In addition, the employment of the corresponding SiD_2 reagent (**2a**−d_2, 95% D) in the coupling with phenylmethanol afforded product **4'**-d with significant H/D exchange (68% D), and analysis of the recovered silane also revealed noticeable Si−H/D exchange (Scheme 4d, 76% D). Next, a series of parallel KIE experiments have been conducted using BnOH−d_5 and/or the SiD_2 silane (Scheme 4e). It was found that the employment of the SiD_2 or the BnOH−d_5 reagent each led to a comparable small kinetic isotope effect (KIE < 1.5). In addition, measuring the initial rates of the silylation of BnOH with **2a** and silylation of BnOH−d_5 with **2a**−d_2 in separate vessels afforded **4** and **4**−d_n in a 1.3:1 ratio. These outcomes indicated that the cleavage of neither the C−H nor the Si−H bond is rate-determining.

Density functional theory (DFT) calculations have been conducted to unravel the origins of enantioselectivity during the formation of the silyl ether intermediate (Figure 2). The computations were performed at the ωB97XD(SMD)/SDD&6-311+G(d,p)//B3LYP-D3(BJ)/SDD&6-31G(d) level of theory (see the computational details in the Supporting Information), with the experimentally employed benzyl alcohol **1** and *tert*-butyl(phenyl)silane **2a** as the model substrates. Considering that essentially the same enantioselectivity of the silyl ether was experimentally observed regardless of the hydrogen acceptor, both possible pathways were thus considered. The computations showed that the enantioselectivity is determined by the same elementary step (*vide infra*). For clarity, in the main text we will focus on the pathway for the absence of the hydrogen acceptor, while the results in the presence of the hydrogen acceptor are provided in the Supporting Information.

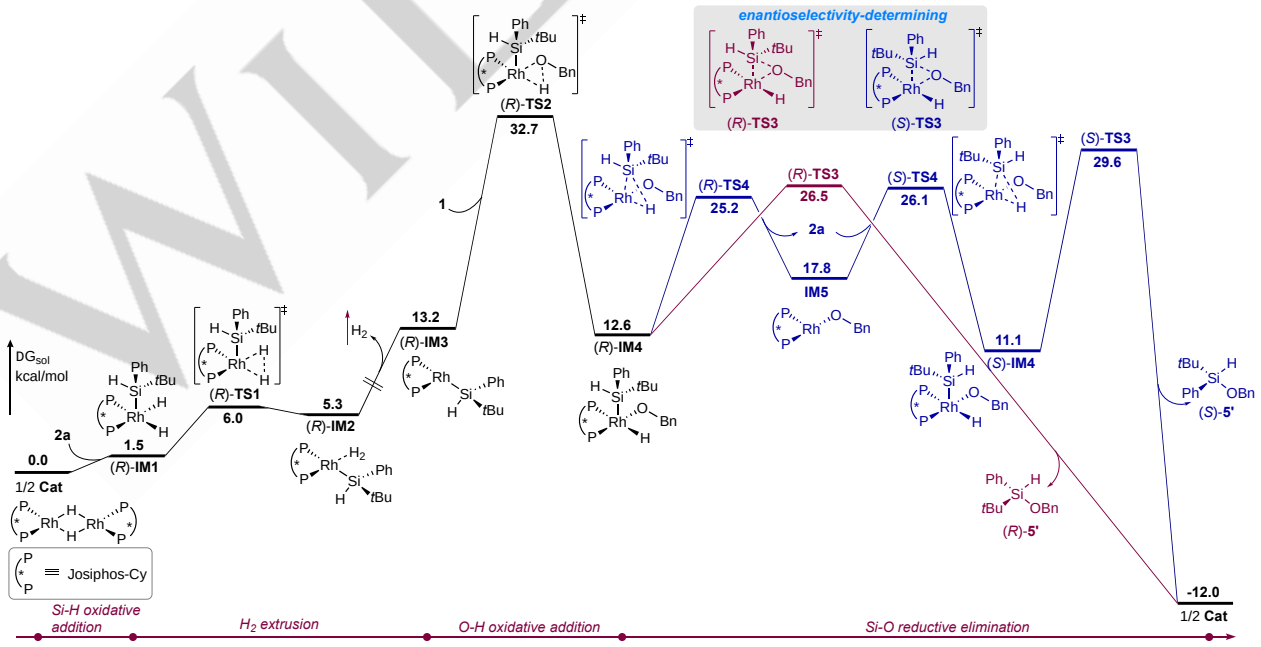

Figure 2. Calculated energy profile for the formation of silyl ether **5'** in the absence of the hydrogen acceptor.

It has been well established that the rhodium(I) chloride pre-catalyst participates in the form of rhodium hydride in dehydrogenative C-H bond silylation based on closely related studies by Hartwig and by He.[22] Thus, Rh(I) hydride species was computationally evaluated in this study.[23] As shown in Figure **2**, the reaction begins with the Si-H oxidative addition to a Rh(I)-H (1/2 **cat.**) to give a Rh(III)-dihydride intermediate (*R*)-**IM1**, which was found to occur with essentially no barrier. Then, (*R*)-**IM1** undergoes the H-H reductive elimination via transition state (*R*)-**TS1** to give H_2-coordinated intermediate (*R*)-**IM2**, with an energy barrier of 4.5 kcal/mol relative to (*R*)-**IM1**. The H_2 extrusion from (*R*)-**IM2** was found to be endergonic by 7.9 kcal/mol, leading to Rh(I)-silyl complex (*R*)-**IM3**. The ensuing O-H oxidative addition with the incoming benzyl alcohol **1** takes place through transition state (*R*)-**TS2**, giving rise to Rh(III)-hydride species (*R*)-**IM4**. It should be emphasized that the irreversibility of the H_2 extrusion divides the entire energy profile into two distinct regimes, namely the pre- and post-H_2 extrusion stages. As a result, the energy barrier of the O-H oxidative addition should be computed relative to (*R*)-**IM3**, which is 19.5 kcal/mol.

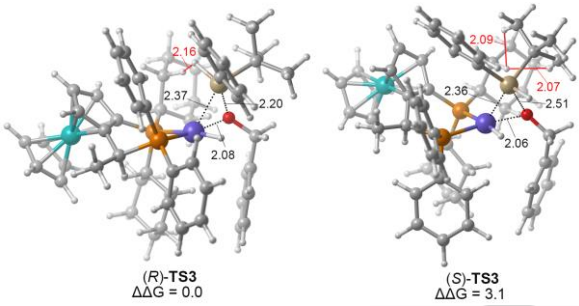

Figure 3. Optimized geometric structures of (*R*)-**TS3** and (*S*)-**TS3**. Energies and bond distances are given in kcal/mol and Å, respectively.

After the formation of Rh(III)-hydride species (*R*)-**IM4**, two possible reaction pathways can be envisioned. The first pathway involves the direct Si-O reductive elimination, occurring through transition state (*R*)-**TS3**, resulting in formation of the experimentally observed silyl ether (*R*)-**5'**. Alternatively, (*R*)-**IM4** can undergo consecutive Si-H reductive elimination (via (*R*)-**TS4**) and reversible Si-H oxidative addition (via (*S*)-**TS4**), leading to the formation of a Rh(III)-hydride (*S*)-**IM4**.[24] From (*S*)-**IM4**, the Si-O reductive elimination proceeds via transition state (*S*)-**TS3**, yielding the minor enantiomer (*S*)-**5'**. The computations showed that the energies associated with the Si-H reductive elimination/oxidative addition are lower than those of the Si-O reductive elimination, in accordance with our deuterium-labelling experiment (Scheme 4d).

It follows that the Si-O reductive elimination serves as the enantio-determining step of the overall reaction. The computed energy difference of 3.1 kcal/mol between (*R*)-**TS3** and (*S*)-**TS3** (26.5 versus 29.6 kcal/mol) corresponds to a predicted d.r. ratio of 98:2 at the specified reaction temperature, which aligns well with experimentally observed enantioselectivity. Detailed analysis of the optimized geometries reveals that the enantioselectivity primarily arises from steric repulsion between the silyl moiety and the Cy group of the ligand Josiphos-Cy (Figure 3). Notably, a more significant steric repulsion was observed in (*S*)-**TS3** (2.07 and 2.09 Å), while in (*R*)-**TS3** the steric repulsion is reduced (2.16 Å), resulting in higher energy of (*S*)-**TS3** when compared to (*R*)-**TS3**.

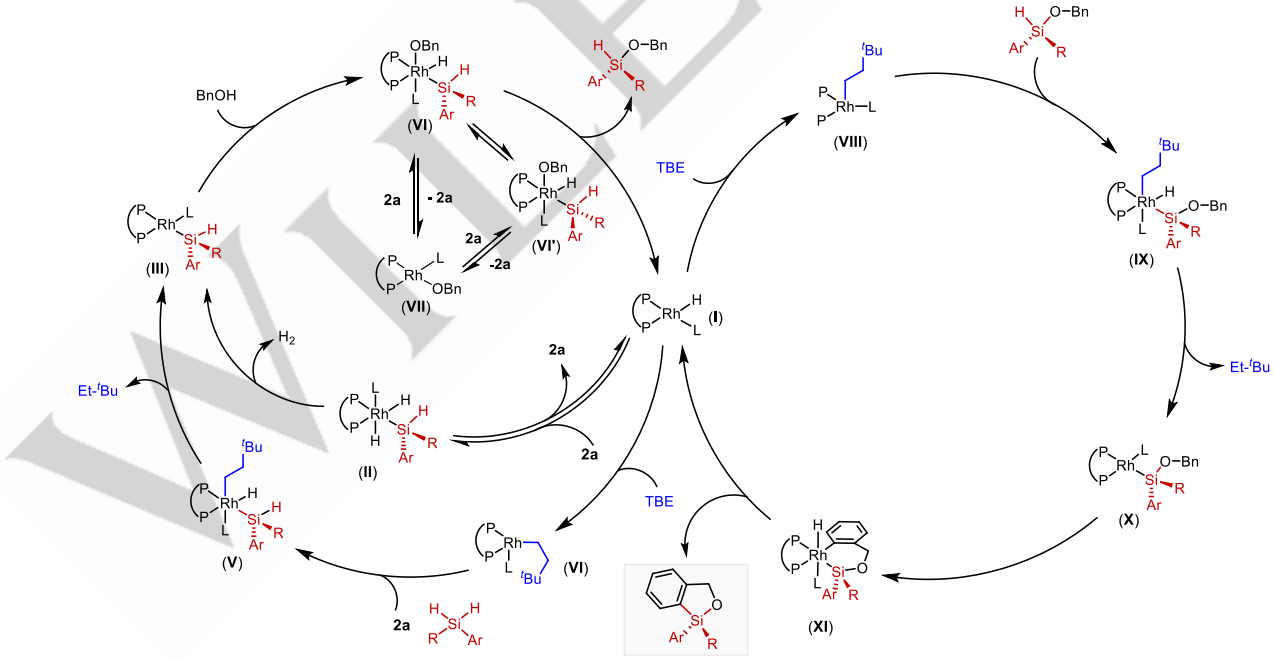

Scheme 5. Proposed mechanism of the reaction of benzyl alcohol.

On the basis of our experimental and DFT studies, a plausible mechanism comprising of two consecutive catalytic cycles is proposed in Scheme 5. In the reaction of benzyl alcohol, facile oxidative addition of the Si−H bond to a Rh(I)-hydride catalyst occurs to give a Rh(III)-dihydride, followed by dihydrogen release via reductive elimination, giving silyl Rh(I) species **III** (Scheme 4c). Alternatively, the initial active Rh(I)-hydride species migratory insertion into TBE generates alkyl rhodium species **VI** (Scheme 5, left). Then, the oxidative addition of Si−H bond and successive reductive elimination of C−H bond

also form silyl Rh(I) species **III** (Scheme 4b). In the catalytic system, both pathways coexist. Coordination and O−H oxidative addition of benzyl alcohol generates a Rh(III)-hydride that may undergo off loop reversible Si−H reductive elimination, accounting for the observed H/D exchange in the silyl ether intermediate and the recovered silane reagent when **2a**-d_2 was used (Scheme 4d). The constructive Si−O reductive elimination produces the silyl ether intermediate with regeneration of the active Rh−H catalyst. In the 2nd catalytic cycle (Scheme 5, right), the rhodium-hydride catalyst is proposed to undergo migratory insertion into the hydrogen acceptor, followed by a 2nd Si−H oxidative addition, affording an alkyl Rh(III)-hydride intermediate. At this stage the rate-limiting C−H reductive elimination produces silyl Rh(I) species **X**.[25] The subsequent silyl-directed C−H activation is proposed to generate alkyl Rh(III)-hydride **XI**, and C−Si reductive elimination furnishes the cyclized product and completes the 2nd catalytic cycle.

Conclusion

In conclusion, we have realized a rhodium-catalyzed asymmetric and intermolecular formal [4+1] sila-cyclization of readily available benzyl alcohols and benzaldimines with secondary silanes, affording chiral-at-silicon cyclic silyl ethers and sila-isoindolines, respectively. A broad scope of simple arene substrates have been defined. Mechanistic studies revealed a dual role of the Rh catalyst that first renders the initial oxygenation or amination of the secondary silane, a process that irreversibly installs a silicon-based directing group, followed by in situ catalytic C−H silylation. Both experimental and DFT studies have been conducted to explore the mechanism of the OH silylation process, and the O-Si reductive elimination has been identified as the enantio-determining step. This work unveils a new protocol for the modular synthesis of silicon-stereogenic sila-heterocycles which will possibly find useful applications in medicinal chemistry.

Acknowledgements

Financial support from the National Key R&D Program of China (No. 2022YFA1503104) and National Natural Science Foundation of China (No. 22073066). S.Y. thanks the Taishan Scholar of Shandong Province (tsqnz20221108) and the Qilu Young Scholar of Shandong University for funding.

Keywords: [4+1] annulation • rhodium asymmetric catalysis • silicon-stereogenic • cyclic silyl ether • silanol

[1] a) E. Langkopf, D. Schinzer, *Chem. Rev.* **1995**, *95*, 1375−1408; b) V. I. Handmann, R.Tacke, *Organometallics* **2003**, *22*, 916−924; c) G. A. Showell, J. S. Mills, *Drug Discov. Today* **2003**, *8*, 551–556; d) R. Tacke, *Organometallics* **2004**, *23*, 4468−4477; e) E. Remond, C. Martin, J. Martinez, F. Cavelier, *Chem. Rev.* **2016**, *116*, 11654−11684. f) d) T. Hiyama, M. Oestreich, *In Organosilicon Chemistry: Novel Approaches and Reactions*, **2019**.

[2] a) M. W. Mutahi, L. Guo, S. M. Sieburth, *J. Am. Chem. Soc.* **2002**, *124*, 7363–7375; b) T. Skrydstrup, *Acc. Chem. Res.* **2013**, *46*, 457−470; c) S. Fujii, *Future Med. Chem.* **2017**, *9*, 485−505.

[3] a) R. Ramesh, D. S. Reddy, *J. Med. Chem.* **2018**, *61*, 3779−3798; b) A. K. Franz, S. O. Wilson, *J. Med. Chem.* **2013**, *56*, 388−405; c) J. Fotie, C. M. Matherne, J. E. Wroblewski, *Chem. Biol. Drug Des*. **2023**, *102*, 35–254; d) F. Chen, L. Liu, W. Zeng, *Front. Chem*. **2023**, *11*, 1200494.

[4] a) R. Bentley, *Chem. Soc. Rev*. **2005**, *34*, 609−624; b) C. A. Holloway, C. J. Matthews, Y.-C. Jeong, M. G. Moloney, C. F. Roberts, M. Yaqoob, *Chem. Biol. Drug Des*. **2011**, *78*, 229−235.

[5] a) N. C. Breit, T. Szilvasi, T. Suzuki, D. Gallego, S. Inoue, *J. Am. Chem. Soc*. **2013**, *135*, 17958−17968; b) L.-W. Xu, L. Li, G.-Q. Lai, J.-X. Jiang, *Chem. Soc. Rev*. **2011**, *40*, 1777−1790.

[6] a) M. Parasram, V. Gevorgyan, *Acc. Chem. Res*. **2017**, *50*, 2038−2053; b) R. Sharma, R. Kumar, I. Kumar, B. Singh, U. Sharma, *Synthesis* **2015**, *47*, 2347−2366; c) C. Cheng, J. F. Hartwig, *Chem. Rev*. **2015**, *115*, 8946–8975; d) B. Li, P. H. Dixneuf, *Chem. Soc. Rev*. **2021**, *50*, 5062−5085; e) Y. Yang, C. Wang, *Sci. China Chem*. **2015**, *58*, 1266−1279; f) L. Zheng, X.-X. Nie, Y. Wu, P. Wang, *Eur. J. Org. Chem*. **2021**, 6006-6014. g) S. C. Richter, M. Oestreich, *Trends in Chemistry* **2020**, *2*, 13−27. h) I. F. Yu, J. W. Wilson, J. F. Hartwig, *Chem. Rev*. **2023**, *123*, 11619–11663.

[7] Y. Kuninobu, K. Yamauchi, N. Tamura, T. Seiki, K. Takai, *Angew. Chem. Int. Ed.* **2013**, *52*, 1520−1522.

[8] T. Shibata, T. Shizuno, T. Sasaki, *Chem. Commun.* **2015**, *51*, 7802−7804.

[9] Q.-W. Zhang, K. An, L.-C. Liu, Y. Yue, W. He, *Angew. Chem. Int. Ed.* **2015**, *54*, 6918−6921.

[10] M. Murai, K. Matsumoto, Y. Takeuchi, K. Takai, *Org. Lett.* **2015**, *17*, 3102−3105.

[11] a) M. Murai, H. Takeshima, H. Morita, Y. Kuninobu, K. Takai, *J. Org. Chem.* **2015**, *80*, 5407–5414; b) M. Murai, Y. Takeuchi, K. Yamauchi, Y. Kuninobu, K. Takai, *Chem. Eur. J.* **2016**, *22*, 6048−6058; c) B. Su, J. F. Hartwig, *J. Am. Chem. Soc.* **2017**, *139*, 12137−12140; d) D. Mu, W. Yuan, S. Chen, N. Wang, B. Yang, L. You, B. Zu, P. Yu, C. He, *J. Am. Chem. Soc.* **2020**, *142*, 13459−13468; e) B. Yang, W. Yang, Y. Guo, L. You, C. He, *Angew. Chem. Int. Ed.* **2020**, *59*, 22217−22222; f) S. Chen, D. Mu, P.-L. Mai, J. Ke, Y. Li, C. He, *Nat. Commun.* **2021**, *12*, 1249-1257; g) Y. Guo, M.-M. Liu, X. Zhu, L. Zhu, C. He, *Angew. Chem. Int. Ed.* **2021**, *60*, 13887−13891; h) W. Ma, L.-C. Liu, K. An, T. He, W. He, *Angew. Chem. Int. Ed.* **2021**, *60*, 4245−4251; i) W. Yuan, L. You, W. Lin, J. Ke, Y. Li, C. He, *Org. Lett.* **2021**, *23*, 1367−1372; j) Y. Sato, C. Takagi, R. Shintani, K. Nozaki, *Angew. Chem. Int. Ed.* **2017**, *56*, 9211−9216.

[12] T. Lee, T. W. Wilson, R. Berg, P. Ryberg, J. F. Hartwig, *J. Am. Chem. Soc.* **2015**, *137*, 6742−6745.

[13] W.-T. Zhao, Z.-Q. Lu, H. Zheng, X.-S. Xue, D. Zhao, *ACS Catal.* **2018**, *8*, 7997−8005.

[14] a) R. Shintani, E. E.Maciver, F. Tamakuni, T. Hayashi, *J. Am. Chem. Soc.* **2012**, *134*, 16955−16958; b) J. Zhu, S. Chen, C. He, *J. Am. Chem. Soc.* **2021**, *143*, 5301−5307. c) D. R. Schmidt, S. J. O'Malley, J. L. Leighton, *J. Am. Chem. Soc.* **2003**,*125*, 1190−1191; d) R. Corriu, J. Moreau, *Tetrahedron Lett*. **1973**, *45*. 4469−4472.

[15] a) C. Cheng, J. F. Hartwig, *Science* **2014**, *343*, 853−857; b) T. Lee, J. F. Hartwig, *Angew. Chem. Int. Ed.* **2016**, *55*, 8723−8727; c) A. Bunescu, T. W. Butcher, J. F. Hartwig, *J. Am. Chem. Soc.* **2018**, *140*, 1502−1507; d) C. Karmel, B. Li, J. F. Hartwig, *J. Am. Chem. Soc.* **2018**, *140*, 1460-1470; e) S. Chen, J. Zhu, J. Ke, Y. Li, C. He, *Angew. Chem. Int. Ed.* **2022**, *61*, e202117820; f) B. Su, J. F. Hartwig, *Angew. Chem. Int. Ed.* **2022**, *61*, e202113343; g) B. Su, T.-G. Zhou, X.-W. Li, X.-R. Shao, P.-L. Xu, W.-L. Wu, J. F. Hartwig, Z.-J. Shi, *Angew. Chem. Int. Ed.* **2017**, *56*, 1092−1096; h) S. Wubbolt, M. Oestreich, *Angew. Chem. Int. Ed.* **2015**, *54*, 15876−15879; i) S. Bahr, M. Oestreich, *Angew. Chem. Int. Ed.* **2017**, *56*, 52−59; j) Y. Fukumoto, M. Hirano, N. Chatani, *ACS Catal.* **2017**, *7*, 3152−3156; k) F. Kakiuchi, N. Chatani, *J. Am. Chem. Soc.* **2004**, *126*, 12792-12793.

[16] Deposition Numbers CCDC 2259271, 2259272, and 2259269 contain the supplementary crystallographic data for this paper. These data are provided free of charge by the joint Cambridge Crystallographic Data Centre and Fachinformationszentrum Karlsruhe Access Structures service.

[17] Q. Li, M. Driess, J. F. Hartwig, *Angew. Chem. Int. Ed*. **2014**, *53*, 8471−8474.

[18] a) T. Daiyo, S. Masato, N. Hiroyuki, *Bull. Chem. Soc. Jpn.* **1982**, *55*, 924−927; b) J. M. Allen, H. Shechter, *J. Org. Chem.* **2002**, *67*, 3561−3574.

[19] H. Fang, W. Hou, G. Liu, Z. Huang, *J. Am. Chem. Soc*. **2017**, *139*, 11601−11609

[20] Employing NBE (1.5 equiv) as a hydrogen acceptor instead of TBE gave comparable results in this control reaction, affording silyl ether **5'** in 83% yield, norbornane in 63%, and recovered NBE in 85% yield.

[21] The coupling of *p*-tolylmethanol and silane **2a** was performed at 50 °C since a low temperature inhibits the cyclization of silyl ether **5'**.

[22] a) T. Lee, J. F. Hartwig, *J. Am. Chem. Soc*. **2017**, *139*, 4879−4886; b) L. Zhang, K. An, Y. Wang, Y.-D. Wu, X. Zhang, Z.-X. Yu, W. He, *J. Am. Chem. Soc.* **2021**, *143*, 3571−3582.

[23] We also computationally evaluated the reaction profile starting from the Rh(I) chloride species. We found that the pathway of Si-H oxidative addition followed by Si-Cl reductive elimination is very feasible, and it is essentially thermoneutral, affording the same rhodium(I) hydride intermediate (1/2 **cat.**) as that given in the Figure 2. In contrast, the pathway of Si-H oxidative addtition followed by HCl reductive elimination is not likely because the subsequent OH oxidative addition of BnOH is kinetically inaccessible. This further supports the plausiblility of rhodium hydride species established in our DFT studies. See Supporting Information for details (Figure S3).

[24] The Rh(III)-hydride species (*S*)-**IM4** can be obtained directly from the (*S*)-pathway of the Si-H oxidative addition/H_2 extrusion/O-H oxidative addition. See the Supporting Information for details.

[25] C. Cheng, J. F. Hartwig, *J. Am. Chem. Soc*. **2014**, *136*, 12064−12072.

10.1002/anie.202315230

Entry for the Table of Contents

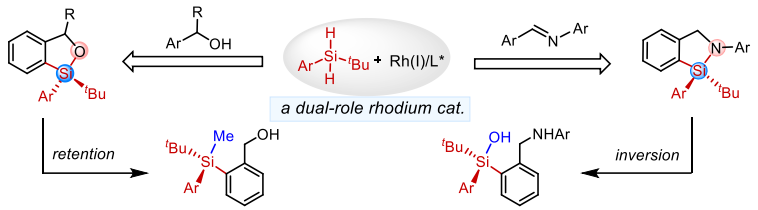

A rhodium-catalyzed enantioselective formal [4+1] annulation of benzyl alcohols and benzaldimines with secondary silanes has been achieved in excellent enantioselectivity to afford a range of sila-*O*- and sila-*N*-heterocycles with silicon-stereogenic centers, where the rhodium catalyst plays a dual role in the O/N−Si and C−Si coupling.